CellPress

Immunity
Article

Continuous T Cell Receptor Signals Maintain a Functional Regulatory T Cell Pool

J. Christoph Vahl,[1,11,13] Christoph Drees,[2,13] Klaus Heger,[1,2] Sylvia Heink,[3] Julius C. Fischer,[2] Jelena Nedjic,[4] Naganari Ohkura,[5] Hiromasa Morikawa,[5] Hendrik Poeck,[2] Sonja Schallenberg,[6] David Rieß,[1,2] Marco Y. Hein,[1,12] Thorsten Buch,[7] Bojan Polic,[8] Anne Schönle,[9] Robert Zeiser,[9] Annette Schmitt-Gräff,[10] Karsten Kretschmer,[6] Ludger Klein,[4] Thomas Korn,[3] Shimon Sakaguchi,[5] and Marc Schmidt-Supprian[1,2,*]

[1]Max Planck Institute of Biochemistry, Am Klopferspitz 18, 82152 Martinsried, Germany
[2]Department of Hematology, Oncology, Klinikum rechts der Isar, Technische Universität München, Ismaninger Straße 15, 81675 Munich, Germany
[3]Department of Neurology, Klinikum rechts der Isar, Technische Universität München, Ismaninger Straße 15, 81675 Munich, Germany
[4]Institute for Immunology, Ludwig-Maximilians University, Goethestraße 31, 80336 Munich, Germany
[5]Department of Experimental Immunology, World Premier International Immunology Frontier Research Center, Osaka University, Suita 565-0871, Japan
[6]Molecular and Cellular Immunology/Immune Regulation, DFG-Center for Regenerative Therapies Dresden (CRTD), Technische Universität Dresden, Fetscherstraße 105, 01307 Dresden, Germany
[7]Institute for Medical Microbiology, Immunology & Hygiene, Trogerstraße 30, Technische Universität München, 81675 Munich, Germany and Institute of Laboratory Animal Sciences, University of Zurich, Winterthurer Straße 190, 8057 Zurich, Switzerland
[8]University of Rijeka School of Medicine, B. Branchetta 20, HR-51000 Rijeka, Croatia
[9]Department of Hematology, Oncology and Stem Cell Transplantation, University of Freiburg, Hugstetter Straße 55, 79106 Freiburg, Germany
[10]Department of Pathology, University Hospital Freiburg, Breisacher Straße 115a, 79106 Freiburg Germany
[11]Present address: Merck Serono, Merck KGaA, Frankfurter Straße 250, 64293 Darmstadt, Germany
[12]Present address: Proteomics and Signal Transduction, Max Planck Institute of Biochemistry, Am Klopferspitz 18, 82152 Martinsried, Germany
[13]Co-first author
*Correspondence: supprian@lrz.tum.de
http://dx.doi.org/10.1016/j.immuni.2014.10.012

SUMMARY

Regulatory T (Treg) cells maintain immune homeostasis and prevent inflammatory and autoimmune responses. During development, thymocytes bearing a moderately self-reactive T cell receptor (TCR) can be selected to become Treg cells. Several observations suggest that also in the periphery mature Treg cells continuously receive self-reactive TCR signals. However, the importance of this inherent autoreactivity for Treg cell biology remains poorly defined. To address this open question, we genetically ablated the TCR of mature Treg cells in vivo. These experiments revealed that TCR-induced Treg lineage-defining Foxp3 expression and gene hypomethylation were uncoupled from TCR input in mature Treg cells. However, Treg cell homeostasis, cell-type-specific gene expression and suppressive function critically depend on continuous triggering of their TCR.

INTRODUCTION

The generation of a peripheral T cell pool with a broad diversity of T cell receptors (TCRs) is critical for a functional immune system. The random nature of somatic TCR gene assembly ensures that a large number of foreign antigens can be recognized. However, this process bears the inherent problem that self-reactive TCRs are also generated. Central and peripheral tolerance mechanisms delete autoreactive T cells or render them ineffective (Xing and Hogquist, 2012). During thymic T cell development, most T cells with a strong self-reactivity to peptide-major histocompatibility complex (MHC) complexes are deleted. Some cells showing intermediate self-reactivity are instructed to develop into regulatory T (Treg) cells, a process known as agonist selection (Josefowicz et al., 2012; Xing and Hogquist, 2012). Treg cells suppress the expansion and function of (autoreactive) effector T cells and their absence or dysfunction leads to severe T cell-mediated pathologies in man and mouse (Josefowicz et al., 2012; Sakaguchi et al., 2008). Treg cells act mostly by suppressing the expansion and function of effector T cells, through various direct and indirect mechanisms.

The key lineage-defining transcription factor Forkhead Box P3 (Foxp3), together with other transcriptional regulators, controls the expression of gene programs necessary to induce and maintain Treg cell identity and function. Foxp3 regulates gene expression mostly in conjunction with other transcriptional regulators, depending on the type of the immune response and the tissue where this response takes place (Fu et al., 2012; Rudra et al., 2012; Stephens et al., 2007). In addition, the establishment of a Treg cell-specific hypomethylation pattern ensures a transcriptionally poised state in a set of Treg cell core genes (Ohkura et al., 2012).

Importantly, these two lineage-defining characteristics of Treg cells, namely Foxp3 expression and the specific hypomethylated state, are induced by rather strong, and in the latter case long-lasting, TCR signals in developing Treg cells. Interruption of

TCR signaling in developing thymic Treg cells by ablation of Lck leads to reduced splenic, but increased lymph node Foxp3$^+$ Treg cell numbers. These Lck-deficient Treg cells display deficiencies in Treg cell signature genes (Kim et al., 2009). Furthermore, a mutation in LAT abolishing its ability to bind to PLCγ1 severely interferes with Treg cell, but not conventional T cell, development (Koonpaew et al., 2006).

Peripheral Treg cell identity depends on continued Foxp3 expression, underscoring its critical importance. Furthermore, the majority of Treg cells express high amounts of CD25, the α chain of the high-affinity IL-2 receptor, and their survival and full Foxp3 expression depends on IL-2 (Josefowicz et al., 2012). The importance of TCR signals for the maintenance of mature Treg cell pool size and lineage identity is less well understood. A reporter mouse for TCR signal strength reveals that Treg cells continuously receive stronger TCR signals than conventional T cells not only during thymic development, but also in the periphery (Moran et al., 2011). However, mice expressing major histocompatibility complex class II (MHCII) glycoproteins only on cortical thymic epithelial cells show normal proportions of CD4$^+$ CD25$^+$ T cells in peripheral lymph nodes (Bensinger et al., 2001), suggesting that homeostasis of mature Treg cells is to a large degree MHCII independent. Furthermore, graded interference in TCR signaling strength by ZAP mutations leads to a reduced number of Treg cells in the thymus, but not in the spleen (Siggs et al., 2007). In contrast, ablation of MHCII expression specifically on CD11c^{hi} dendritic cells significantly reduces proportions and the absolute number of Treg cells in lymph nodes and spleen (Darrasse-Jèze et al., 2009).

To directly address the importance of tonic TCR signaling for peripheral Treg cell homeostasis and lineage identity, we monitored the consequences of induced TCR ablation on mature Treg cells. Our results show that although TCR-deficient Treg cells maintain Foxp3 expression and their lineage-specific hypomethylation pattern, continuous TCR signals are required to maintain their activated phenotype, homeostasis, and their immunosuppressive properties. Therefore, we propose that TCR-derived signals are not only critical during thymic development, but also for the maintenance and function of peripheral Treg cells.

RESULTS

Foxp3 Expression Is Independent of Continuous TCR Signals in Mature Peripheral Treg Cells

In order to study the importance of TCR signaling for Treg cells in vivo, we ablated the TCRα chain by poly(I:C) injection of *Mx1-cre Tcra*$^{F/F}$ mice. This leads to downregulation of TCRβ-chain and CD3 surface expression after 5 days and nearly complete surface absence of both molecules after 10 days (Polic et al., 2001). Two weeks after poly(I:C) treatment, around 25% of the Foxp3$^+$ Treg cells had lost TCR surface expression (see Figure S1A available online). To facilitate the identification of Treg cells, *Mx1-cre Tcra*$^{F/F}$ mice were bred to the Foxp3-I-eGFP reporter strain (Bettelli et al., 2006), in which GFP expression reports *Foxp3* mRNA amounts (*Tcra*$^{F/F}$ stands for *Tcra*$^{F/F}$ and *Tcra*$^{F/F}$ Foxp3-I-eGFP throughout the manuscript). We analyzed Treg cells 6 weeks after induced TCR ablation unless otherwise indicated, so that they lacked TCR signals for at least 1 month. Our analyses were conducted mostly with thymus-derived Treg cells, because we detected only very low numbers of Nrp1^{lo} peripherally derived pTreg cells in the spleen (Figure S1B). Importantly, 6 weeks after TCR loss, TCR-deficient Treg cells still expressed high Foxp3 amounts and were exclusively CD25^{hi} (Figures 1A–1C and S1C and S1D). Analyses of *Mx1-cre* mT/mG reporter mice (Muzumdar et al., 2007) revealed equal Cre-mediated recombination efficiencies in various Treg cell subsets, including CD25^{lo} Treg cells, at this time point (Figure S1E). This indicates that CD25^{lo} Treg cells were either lost or upregulated CD25 after TCR ablation. Because CD25^{hi} and CD25^{lo} Treg cells differ in their gene expression and proliferation (Fontenot et al., 2005), we compared CD25^{hi} TCR-deficient to TCR-expressing CD25^{hi} Treg cells unless stated otherwise. Foxp3 protein levels of TCR$^-$ (CD25^{hi}) Treg cells were slightly reduced (10%) in comparison to TCR$^+$ CD25^{hi} Treg cells, but still significantly higher than those of TCR$^+$ CD25^{lo} Treg cells (Figures 1A and S1C). GFP amounts reporting *Foxp3* mRNA were virtually identical between TCR$^+$ CD25^{hi} and TCR$^-$ Treg cells (Figures 1B and S1D). This indicates that TCR signals induce posttranslational stabilization of the Foxp3 protein. GFP-expression and hence *Foxp3* mRNA amounts remain stable in all TCR$^-$ Treg cells at 4, 8, or 12 days after induced TCR ablation while Foxp3 protein amounts decrease to their final levels within 8 days (Figures S1F and S1G).

Together, these experiments demonstrate that continuous TCR signals are largely dispensable for the maintenance of Foxp3 expression of mature Treg cells.

The Treg Cell-Specific Epigenetic Pattern Is Not Affected by TCR Ablation

Besides Foxp3 expression, the establishment of a specific hypomethylation pattern (nTreg-Me), especially within the gene loci of *Foxp3*, *Gitr*, *Ctla4*, and *Ikzf4 (*Eos), is of critical importance during thymic Treg cell development (Ohkura et al., 2012). Long-lasting TCR stimulation of developing thymocytes is shown to induce nTreg-Me whereas Foxp3 expression is a consequence of strong TCR activation (Ohkura et al., 2012). Bisulfite sequencing of purified TCR-deficient and proficient Treg cells 6 and 15 weeks after poly(I:C)-induced TCR ablation did not reveal changes in the Treg cell-specific methylation pattern (Figure 1D). In line with this finding, the protein amounts of genes that contain hypomethylated regulatory regions were, albeit reduced, still significantly higher in TCR-deficient Treg cells than in naive conventional T cells (Figures 1A, 1E, and 2D). Furthermore, we also did not detect major differences in the mRNA expression levels of several additional genes containing Treg cell-specific DNA demethylated regions (Morikawa et al., 2014) (Figure S1H).

These results demonstrate that maintenance of the Treg cell-specific methylation pattern is completely independent of continuous TCR signals. Hypomethylation therefore uncouples the expression of key Treg cell genes from obligate TCR signals to a large extent.

TCR Signals Continuously Activate Peripheral Treg Cells

The peripheral Treg cell pool contains naive and effector or tissue-homing subsets (Campbell and Koch, 2011; Fisson et al., 2003). Naive Treg cells are quiescent and express

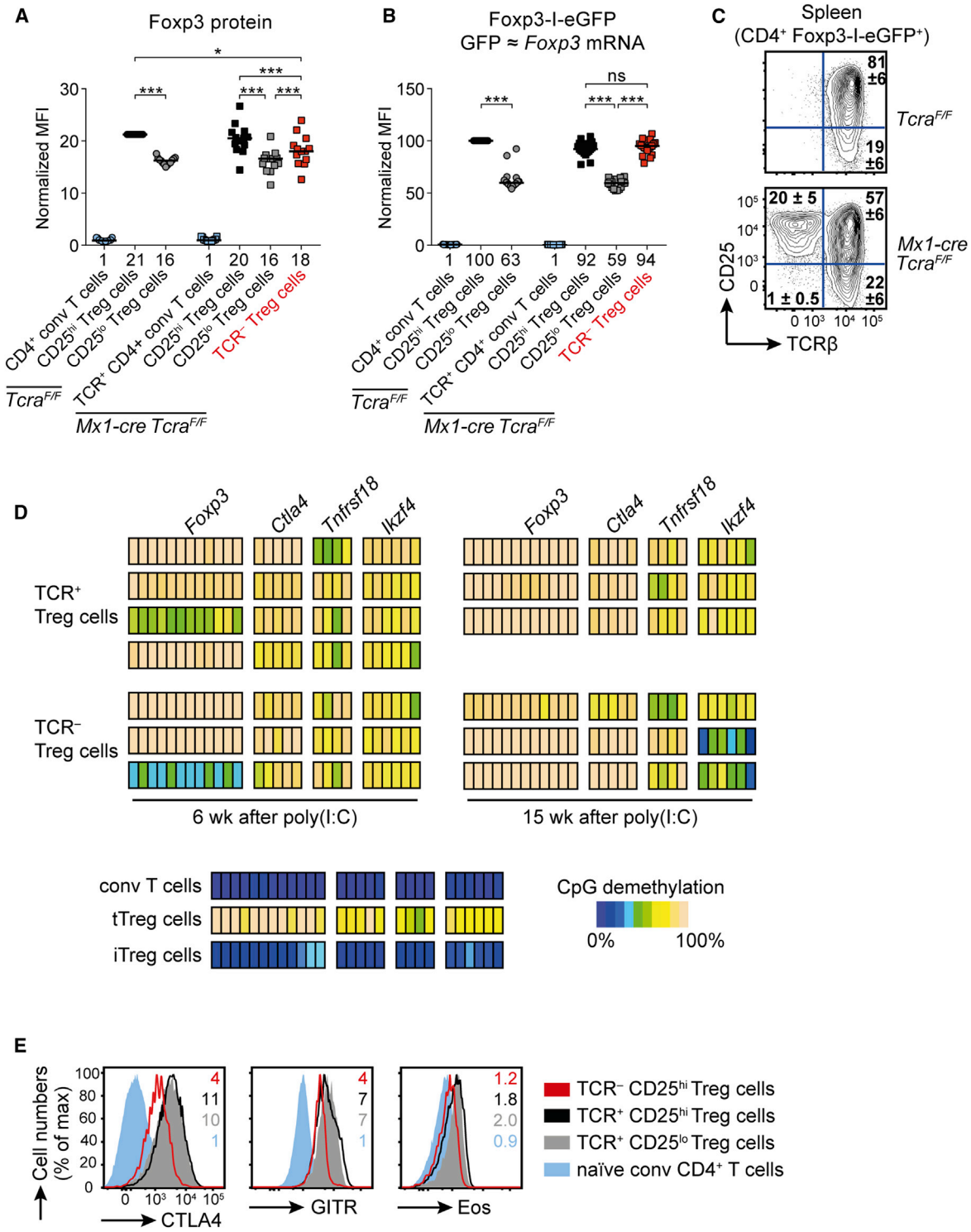

Figure 1. Foxp3 Protein Expression and Treg Cell-Specific Methylation Pattern Remain in Absence of TCR Signals

(A and B) Intracellular Foxp3 expression (A) and Foxp3-I-eGFP expression (B) 6 weeks after poly(I:C) injection. Median fluorescence intensities (MFI) were normalized to CD25^{hi} Treg cells of *Tcra*$^{F/F}$ animals, then set to 1 for CD4^{+} conventional T cells (A), or normalized to CD25^{hi} Treg cells of *Tcra*$^{F/F}$ animals in percentage (B). Numbers below the plot indicate means of the normalized MFIs and were calculated from 10 mice per genotype from 4 independent experiments (A) and from 16 mice per genotype from 5 independent experiments (B). ***$p < 0.001$; *$p < 0.05$; ns, not significant; one-way ANOVA.

(C) Surface CD25 and TCRβ expression on Foxp3-I-eGFP^{+} Treg cells 6 weeks after poly(I:C) injection. Numbers indicate mean percentage ± SD of ≥ 14 mice per genotype from ≥ 4 independent experiments.

(legend continued on next page)

CD62L and the chemokine receptor CCR7, enabling them to enter secondary lymphoid organs (Campbell and Koch, 2011). In contrast, effector Treg cells are cycling and show increased expression of CD5, CD38, CD44, Ox40, GITR, CD69, and ICAM-1 (Campbell and Koch, 2011; Feuerer et al., 2009; Fisson et al., 2003; Fontenot et al., 2005; Huehn et al., 2004; Stephens et al., 2007). A direct comparison of the CD25^{hi} to the CD25^{lo} Treg cell subsets reveals that the CD25^{lo} subset is enriched for proliferating cells expressing effector markers (Fontenot et al., 2005). It was proposed that the effector Treg cell subset is comprised of short-lived cells that were recently activated by (self-)antigens (Campbell and Koch, 2011; Fisson et al., 2003).

TCR ablation did not reduce the proportions of Treg cells expressing CCR7 and CD62L, suggesting that TCR-deficient Treg cells can recirculate efficiently between secondary lymphoid organs (Figure S2A). In contrast, we observed that activation and/or effector markers such as 4-1BB, CD49b, CD69, PD-1, and KLRG1 were virtually absent on TCR-deficient Treg cells (Figure 2A).

To further elucidate the impact of TCR signals for Treg cell identity, we monitored the protein amounts of well-described Treg cell markers after TCR ablation. Our analysis revealed that surface amounts of the costimulatory molecules ICOS, CD28, and Ox40, as well as of CD38, CD44, CD5, ICAM-1, and TIGIT, were significantly decreased, whereas CD45RB was upregulated (Figures 2B and S2B). Fittingly, relative quantification of intracellular transcription factor protein amounts showed that Egr2, c-Rel, and c-Maf, which have been linked to TCR activation, were dramatically downregulated (Figures 2C and 2D). The expression of several other important transcription factors connected to Treg cell function (Fu et al., 2012; Rudra et al., 2012) such as IRF4, Helios, GATA3, KLF4, T-bet, and Aiolos, but not Runx1 and Bcl-6, was significantly reduced in the TCR-deficient cells, although not to the amounts found in naive CD4$^+$ T cells (Figures 2C, 2D, and S2C). A comprehensive overview of surface-marker proteins and transcription factors analyzed by flow cytometry is shown in Figure 2D.

We then assessed the dynamic changes in protein levels of selected markers 4, 8, and 12 days after TCR ablation. At day 4 TCR downregulation was similar in all tested Treg cell subsets, including CD25^{lo}, CD69^{hi}, and CD103$^+$ (Figure S2D), confirming equal TCR ablation efficiencies between different Treg cell subsets. The TCR-deficient effector Treg cell subsets slowly shrank in size, with the exception of the CD103$^+$ subset (Figures S2E and S2F). Over time, TCR-deficient Treg cells gradually lost TCR-dependent surface marker and transcription factor expression (Figures 2E and S2G–S2I). This occurred on CD25^{hi} and as long as they persisted also on CD25^{lo} subsets (Figure S2H) and on individual effector subset defined by high-marker protein expression (Figure S2I). We did not detect increased proportions of dead or dying Treg cells at any time point after TCR ablation by propidium iodide and Annexin V staining (Figure S2J). Therefore, individual Treg cell effector subsets are slowly disappearing in response to TCR ablation, and this goes hand-in-hand with loss of typical gene expression.

We conclude that de novo differentiation and maintenance of effector Treg cell subset phenotypes cannot occur in absence of TCR signals. Furthermore, our analysis of effector-type and "naive" CD25^{hi} TCR-deficient Treg cells showed a substantial loss of lineage-defining protein expression. However, although in absence of TCR signals the protein amounts of some activation markers and transcription factors were reduced to amounts found on naive conventional CD4$^+$ T cells, the majority of proteins were present at amounts in between conventional CD4$^+$ T and Treg cells.

TCR-Dependent Gene Expression in Treg Cells Is Dominated by TCR-Induced Transcription Factors and IRF4

To examine the consequences of the loss of TCR signals globally, we analyzed gene-expression changes through Affymetrix microarrays. In total, loss of the TCR affected the expression of 327 genes at least 2-fold and of 65 genes at least 3-fold in CD25^{hi} Treg cells. The majority of these genes were downregulated (71% of the 2-fold regulated genes and 68% of the 3-fold regulated genes); this included genes encoding for cell surface molecules such as 4-1BB (encoded by *Tnfrsf9*), CD38, ICOS, and PD-1 (encoded by *Pdcd1*) as already observed by flow cytometry (Figures 2A–2D and Table S1).

TCR ablation affected various gene subsets (defined in Table S2): Of Treg cell signature genes, 15 (4%) were significantly reduced to less than $^1/_3$ and 135 (30%) were reduced to less than $^2/_3$ of their expression in TCR$^+$ Treg cells, while only a minor fraction was upregulated (Figure 3A). This indicates that while a proportion of the characteristic Treg cell gene expression relies at least partially on TCR-derived signals, overall TCR-deficient Treg cells maintain their cellular identity.

In agreement with the persistent Foxp3 protein amounts in TCR-deficient Treg cells, Foxp3-regulated genes were not strongly affected. Nevertheless, over 30% of the Foxp3-activated genes in TCR-deficient Treg cells were reduced to less than $^2/_3$ of their expression in TCR$^+$ Treg cells (Figure 3B), defining a candidate set of Foxp3-activated genes that require TCR signals for full expression. Consistent with the dramatic loss of Egr2 expression upon TCR ablation, we detected a significant reduction in Egr2-dependent gene expression (Figure 3C). A set of general NF-κB target genes was equally up- and downregulated (Figure S3A). However, genes whose expression was reduced in c-Rel-deficient activated T cells were mostly downregulated upon TCR ablation (Figure 3D), underscoring the unique role of c-Rel among the NF-κB transcription factors in Treg cells. GATA3- or Runx1-controlled gene expression remained stable in TCR-deficient Treg cells, as none of them were significantly regulated more than 2-fold (data not shown). An analysis of putative NFAT target genes revealed that 30% depend to some extent on TCR signals in Treg cells (Figure 3E). Among

(D) CpG methylation status of splenic CD25^{hi} TCR$^+$ and TCR$^-$ Foxp3$^+$ Treg cells, 6 weeks or 15 weeks after poly(I:C) injection. tTreg = thymus-derived Treg; iTreg = in vitro-induced Treg.

(E) Intracellular (CTLA4, Eos) or extracellular (GITR) expression of the indicated splenic T cell subsets (Treg = Foxp3$^+$), all from *Mx1-cre Tcra*$^{F/F}$ mice 6 weeks after poly(I:C) injection. Numbers in representative histograms indicate means of the MFIs, normalized to Foxp3$^-$ CD4$^+$ CD44^{lo} naive T cells of *Tcra*$^{F/F}$ mice. Means were calculated from ≥ 5 mice per genotype from ≥ 2 independent experiments. See also Figure S1.

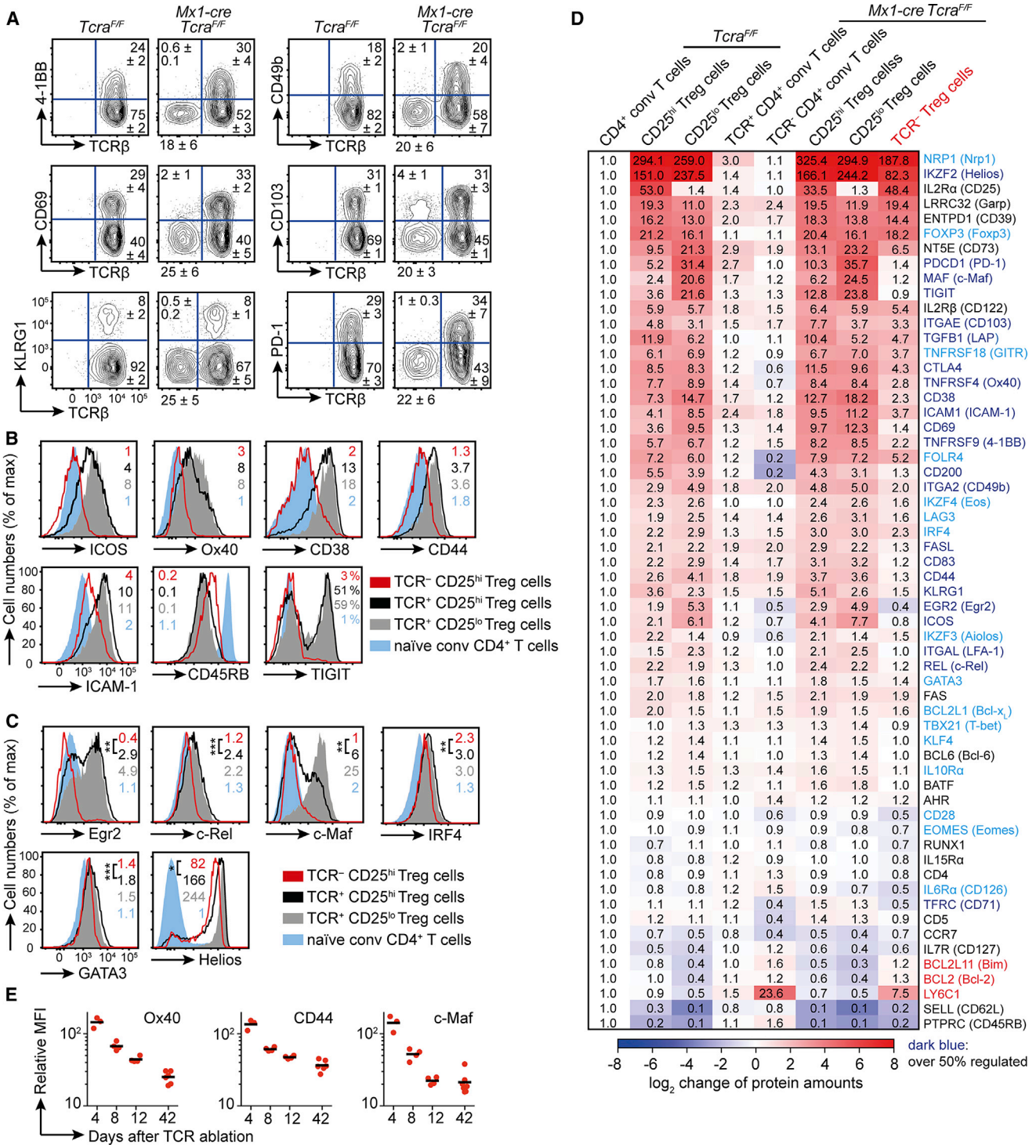

Figure 2. TCR-Deficient Regulatory T Cells Lose Their Activated Phenotype

(A) Extracellular expression of the depicted markers on splenic Foxp3-I-eGFP^{+} CD25^{hi} Treg cells, 6 weeks after poly(I:C) injection. Numbers in representative plots indicate mean percentage ± SD of 6–13 mice per genotype from ≥ 2 independent experiments.

(B and C) Extracellular (B) or intracellular (C) expression of the depicted markers of the indicated splenic T cell subsets (Treg = Foxp3^{+}), all from *Mx1-cre Tcra*$^{F/F}$ mice 6 weeks after poly(I:C) injection. Numbers in representative histograms indicate means of the MFIs, normalized to Foxp3^{-} CD4^{+} CD44^{lo} naive T cells of *Tcra*$^{F/F}$ mice. For TIGIT, percentage of positive cells are shown. Means were calculated from ≥ 5 mice per genotype from ≥ 2 independent experiments. ***p < 0.001; **p < 0.01; *p < 0.05; one-way ANOVA.

(D) Flow cytometric protein level analysis of extra- and intracellular markers of splenic T cell subsets (Treg = Foxp3^{+}) 6 weeks after poly(I:C) injection. MFIs of ≥ 3 mice per analyzed protein were normalized to the expression on or in conventional CD4^{+} T cells to account for interexperimental variations. Data are shown as

(legend continued on next page)

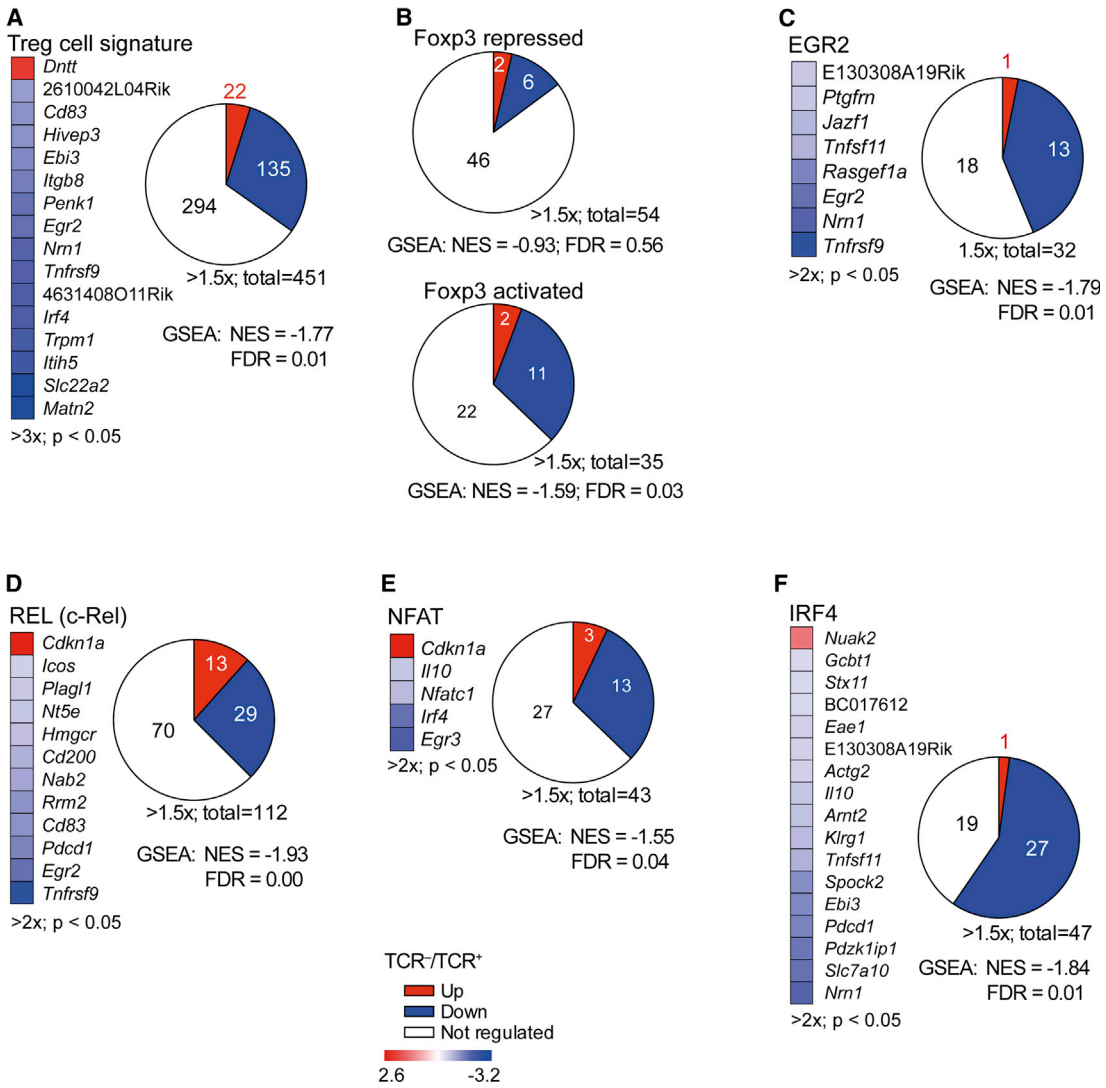

Figure 3. Treg Cell mRNA Expression Is Severely Changed upon TCR Ablation

(A–F) The mRNA expression of splenic Foxp3-I-eGFP$^+$ TCR$^+$ CD25^{hi} Treg cells from 4 *Tcra*$^{F/F}$ control samples (WT) and Foxp3-I-eGFP$^+$ TCR$^-$ CD25^{hi} Treg cells from 5 *Mx1-cre Tcra*$^{F/F}$ samples (KO), 6 weeks after poly(I:C) injection, was compared by Affymetrix microarray. Each sample contained pooled Treg cells from 3-5 mice. Normalized enrichment scores (NES) were calculated at the indicated false discovery rate (FDR) at the GSEA server of the Broad Institute. Changes in the expression of (A) Treg cell signature genes and (B) direct Foxp3 target genes that are either repressed (top; less than ½ of expression in TCR$^+$ Treg cells: *Tbc1d4*) or activated (bottom; less than ½ of expression in TCR$^+$ Treg cells: *Icos*) upon Foxp3 promoter occupancy. Changes in putative target gene expression of (C) Egr2, (D) REL (c-Rel), (E) NFAT transcription factors, and (F) IRF4 are shown. Pie charts show the number of detected genes within the respective category (white, not regulated; red, ≥ 1.5-fold upregulated; blue, $^2/_3$ of the expression in TCR$^+$ Treg cells) in KO relative to WT Treg cells. Heatmaps depict knockout (KO) to WT fold-change values (Log2-transformed; A, ≥ 3-fold; B–F, ≥ 2-fold) of significantly regulated genes ($p < 0.05$; t test). See also Figure S3 and Tables S1 and S2.

the significantly downregulated NFAT and c-Rel target genes were Egr2, Egr3, and IRF4 (Figures 3D, 3E, and S3B), suggesting a TCR-dependent transcription-factor network. Although IRF4 protein amounts were only reduced by around 20%, TCR ablation had the largest effect on IRF4-controlled gene expression: 57% of the 47 IRF4 target genes were downregulated to less than 2/3 of their expression in TCR$^+$ Treg cells, 16 (34%) of which statistically significantly to less than ½ (Figure 3F). Gene-set enrichment analysis (GSEA) confirmed significant (FDR ≤ 0.05) loss of Treg signature genes and Foxp3 activated, Egr2, c-Rel, NFAT, and IRF4 target genes in TCR-deficient Treg cells (Figure 3 and Table S2). Unbiased analysis of the gene-expression data from TCR-deficient and control Treg cells against publicly available gene sets suggested loss of Egr3 and Egr2 target genes,

heatmap (Perseus software). Blue letters, significantly ($p < 0.05$) reduced on or in TCR$^-$ Treg cells in comparison to TCR$^+$ CD25^{hi} Treg cells from both *Tcra*$^{F/F}$ control, as well as *Mx1-cre Tcra*$^{F/F}$ mice. Red letters, significantly increased ($p < 0.05$); analyzed by one-way ANOVA.

(E) Decay of the indicated proteins after TCR ablation. Shown are MFIs of TCR-deficient relative to MFI of TCR$^+$ Foxp3$^+$ Treg cells. Depicted are values for individual mice and means. See also Figure S2.

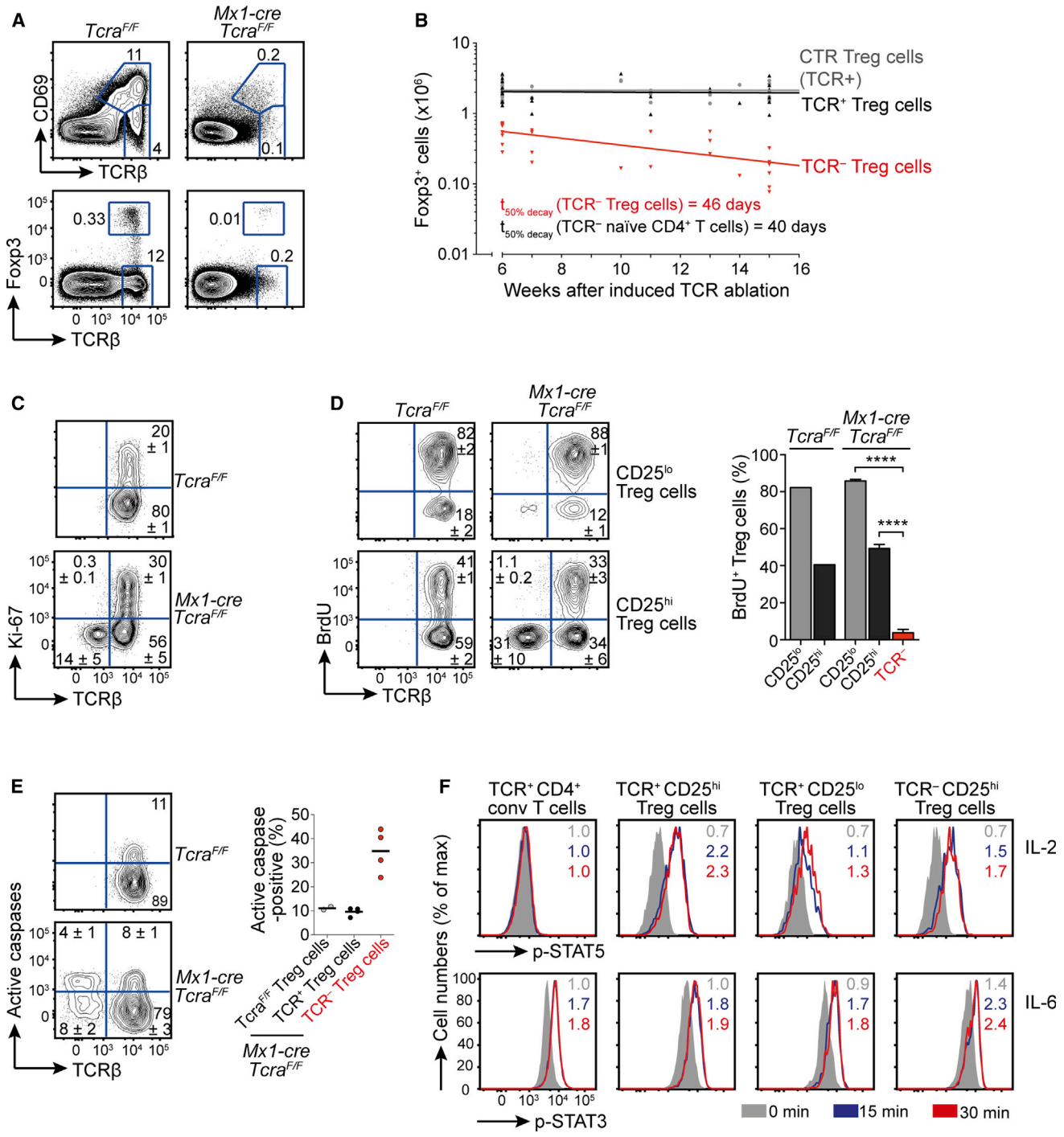

Figure 4. Regulatory T Cell Homeostasis Is Impaired upon TCR Ablation

(A) Expression of CD69 and Foxp3 plotted against TCRβ on total thymocytes, 6 weeks after poly(I:C) injection. Plots are representative of five independent experiments.

(B) Number of splenic Foxp3$^+$ Treg cells from in total 24 control (CTR) *Tcra*$^{F/F}$ mice, as well as number of TCR$^+$ and TCR$^-$ Treg cells from in total 23 *Mx1-cre Tcra*$^{F/F}$ mice from 14 independent experiments, at the indicated time after poly(I:C) injection. $t_{50\%\ decay}$ = time it takes until the population decayed to half of its size.

(C) Intracellular expression of Ki-67 in splenic Foxp3$^+$ Treg cells, 6 weeks after poly(I:C) injection. Numbers in representative plots indicate mean percentage ± SD of 4 mice per genotype and are representative for 3 independent experiments.

(D) BrdU was administered for 4 weeks via the drinking water, starting 2 weeks after poly(I:C) injection. Directly afterward, BrdU incorporation in CD25^{lo} and CD25^{hi} Foxp3$^+$ Treg cells was measured by flow cytometry. Numbers in representative plots indicate mean percentage ± SD of 2–4 mice per genotype. Bar chart depicts means + SD of one experiment with 2 *Tcra*$^{F/F}$, as well as 4 *Mx1-cre Tcra*$^{F/F}$ mice. ****p < 0.00001; one-way ANOVA.

(legend continued on next page)

loss of Foxp3 amplified genes, and a shift toward gene expression of conventional T cells (Figure S3C).

The overwhelming majority of differentially expressed mRNAs were downregulated in TCR-deficient Treg cells, indicating that a large part of the Treg cell-specific gene-expression pattern depends on autoreactive TCR signals. This TCR-dependent gene expression appears to depend on Egr2, Egr3, c-Rel, and most prominently, IRF4. However, TCR-deficient Treg cells globally maintain their transcriptional identity.

The Peripheral Homeostasis of Treg Cells Requires TCR Signals

Having established that TCR signals are indispensable for the differentiation and maintenance of effector Treg cells and critical for the expression of many Treg lineage-defining genes, we wanted to assess the role of TCR signals for "naive" $CD25^{hi}$ Treg cell maintenance. Upon poly(I:C) treatment, T cell development is blocked in *Mx1-cre* $Tcra^{F/F}$ mice, due to complete TCRα inactivation in lymphoid progenitors (Figure 4A). Therefore, we employed these mice to study the homeostasis of peripheral Treg cells in the absence of cellular efflux from the thymus. The population of TCR^- Treg cells decayed (Figure 4B), similar to TCR-deficient naive $CD4^+$ cells, but in stark contrast to $CD4^+$ $CD44^{hi}$ memory and effector T cells and $CD4^+$ natural killer T (NKT) cells, which rely on cytokines but not on TCR stimulation (Polic et al., 2001; Vahl et al., 2013). The total number of peripheral Treg cells was not changed significantly 6 weeks and 15 weeks after induced TCR ablation, unlike the number of naive $CD4^+$ and $CD8^+$ T cells (Figures 4B and S4A). Thus, the peripheral Treg cell pool size is kept stable in the absence of thymic output.

The decrease of peripheral TCR-deficient Treg cells (Figure 4B) could be a consequence of impaired survival and/or proliferation. The proliferation marker Ki-67 was not expressed by TCR-deficient Treg cells (Figure 4C). In order to directly monitor the proliferation of Treg cells in the absence of TCR signals, mice containing TCR-deficient and -proficient Treg cells received BrdU-containing water for 4 weeks. Over 80% of $CD25^{lo}$ Treg cells, as well as 40%–50% of TCR^+ $CD25^{hi}$ Treg cells incorporated BrdU during this time (Figure 4D). The BrdU-incorporation of TCR-deficient Treg cells was negligible, demonstrating that homeostatic Treg cell proliferation absolutely requires tonic TCR signals (Figure 4D).

Direct ex vivo analyses suggested that loss of the TCR has no major impact on the survival of Treg cells (Figure S2J). However, a significantly higher percentage of TCR-deficient Treg cells contained activated caspases (Figure 4E) after 1 hr in cell culture, indicating that in vitro, TCR-deficient Treg cells have an increased tendency to undergo apoptosis.

Cytokines, most importantly IL-2 and IL-7, influence the homeostasis of Treg cells (Setoguchi et al., 2005). While all TCR-deficient Treg cells expressed high amounts of CD25 (Figure 1C), expression of CD122 (IL-2R and IL-15R β chain), CD127 (IL-7Rα chain), and the IL-15Rα chain were not significantly altered upon TCR ablation (Figures 2D and S4B). Importantly, TCR-deficient Treg cells were competent in cytokine signaling as evidenced by robust phosphorylation of STAT5 and STAT3 transcription factors in response to IL-2 and IL-6 stimulation (Figure 4F). In addition, the homeostatic defects of TCR-deficient Treg cells appeared unrelated to endoplasmic reticulum (ER) stress caused by an unpaired TCRβ chain because we did not detect major alterations in the expression of genes implicated in the endoplasmic reticulum associated degradation (ERAD) and in the unfolded protein response pathways (Table S2).

Together, these results demonstrate that the absence of TCR signals effectively abrogates Treg cell homeostasis, due to essentially abolished proliferation.

Elevated mTOR Signaling in Treg Cells Is TCR Mediated

Signals derived from antigen recognition, costimulation, cytokines, growth hormones, and nutrients converge on the mechanistic target of rapamycin (mTOR) pathway. Signaling through its two multiprotein complexes, mTORC1 and mTORC2, and the upstream kinase AKT regulates cellular growth, protein translation, and survival in many cell types, including T cells (Chi, 2012). Importantly, Treg cells contain and depend on enhanced mTORC1 signaling for their homeostasis and function (Zeng et al., 2013).

We detected lower phosphorylation of mTOR and its targets ribosomal protein S6, kinase p70 S6, the translational inhibitor 4E-BP1, and reduced expression of the mTORC1 target CD71 in TCR^- Treg cells (Figures 5A, 5B, and S5A–S5C). We also detected a trend toward downregulation of mTORC1 target genes controlling the cholesterol biosynthesis pathway (Figures 5C and S5D), which has a central role in Treg cells (Zeng et al., 2013). In contrast, we did not observe differences in mTORC1-controlled mitochondrial parameters including their reactive oxygen production, membrane potential, and mass (Figure S5E) (Zeng et al., 2013).

mTORC2 plays an important role in the inhibition of apoptosis by directly phosphorylating the kinase AKT at serine 473, enabling it to phosphorylate and thereby inhibit constitutively active FoxO transcription factors. TCR-deficient Treg cells contained strongly reduced AKT-S473 phosphorylation (Figure 5D) and correspondingly reduced FoxO1 phosphorylation at the AKT target site serine 256, but not protein amounts (Figures 5E and S5F). The proapoptotic BH3-only protein Bim, a FoxO target in T cells (Hedrick et al., 2012), was significantly increased upon TCR ablation (Figures 2B and 5F). Moreover, we observed decreased amounts of the antiapoptotic protein Bcl-xL in TCR-deficient Treg cells. On the other hand, the amounts of the antiapoptotic protein Bcl-2 were significantly elevated, possibly due to mutual posttranslational control with Bim (Jorgensen et al., 2007) (Figures 2B and 5F). Finally, inhibitory phosphorylation of the proapoptotic Bcl-2 family member Bad, an AKT target (del Peso et al., 1997), was reduced (Figure 5F). However, globally

(E) Splenic $Foxp3^+$ Treg cells were stained in vitro for 1 hr for the presence of active caspases. Numbers indicate mean percentage ± SD of 2 $Tcra^{F/F}$ or 4 *Mx1-cre* $Tcra^{F/F}$ mice. Scatterplot shows the percentage of active $caspase^+$ $Foxp3^+$ Treg cells from 2 control $Tcra^{F/F}$ or from 4 *Mx1-cre* $Tcra^{F/F}$ mice. Bars indicate means. (F) Comparison of STAT5 and STAT3 phosphorylation upon stimulation with IL-2 or IL-6 of the indicated T cell subsets from *Mx1-cre* $Tcra^{F/F}$ mice. Numbers in representative histograms indicate means of the MFIs, normalized to unstimulated $Foxp3^-$ $CD4^+$ $CD25^{lo}$ TCR^+ T cells. Means were calculated from 6 mice from 2 independent experiments (p-STAT5) or from 3 mice (p-STAT3). See also Figure S4.

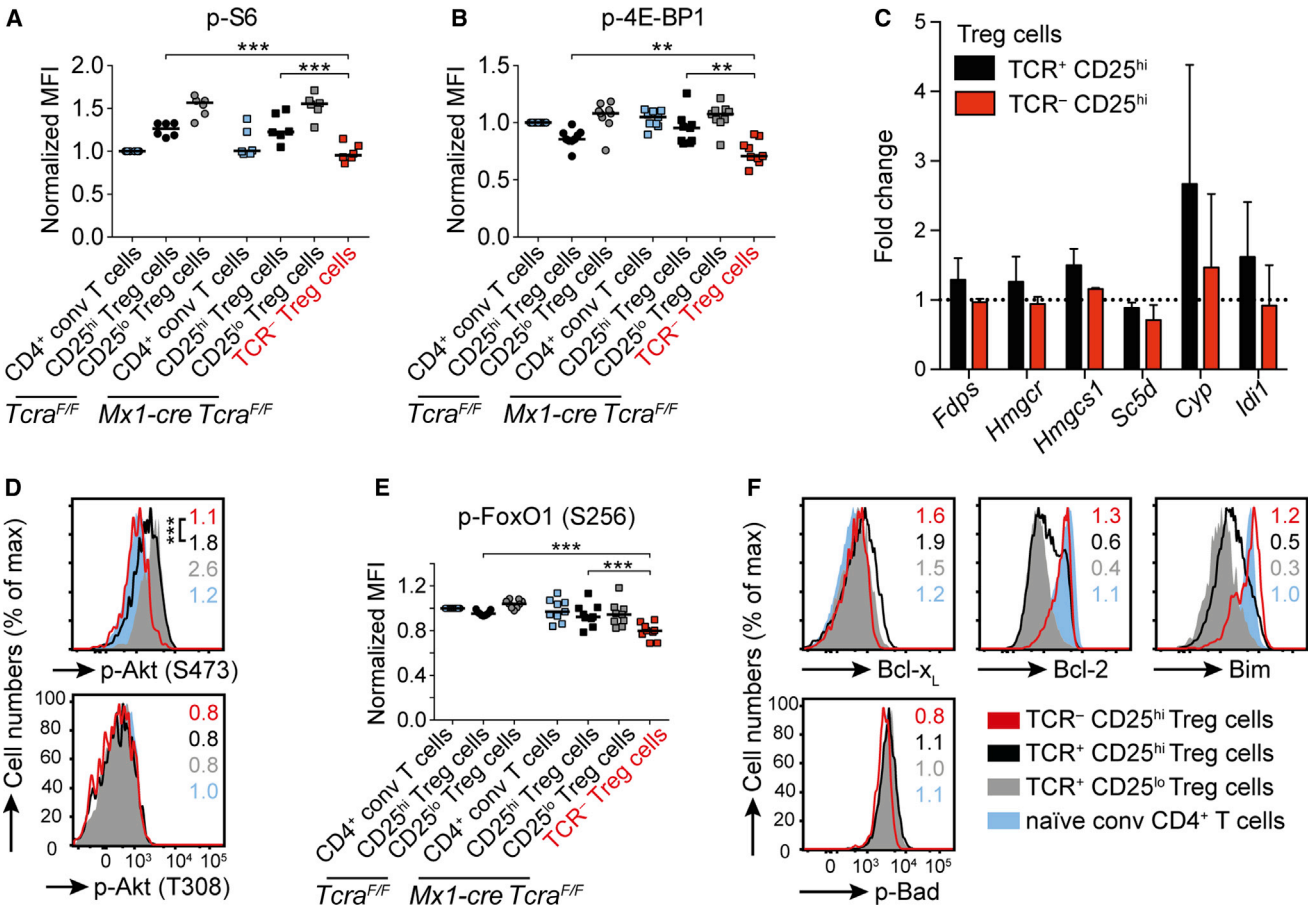

Figure 5. mTOR Signaling Pathways Are Attenuated in TCR-Deficient Treg Cells

(A, B, D, E, and F) Comparison of phosphorylation or expression of the respective proteins in the indicated splenic T cell subsets (Treg = Foxp3$^+$) 6 weeks after poly(I:C) injection. Numbers in representative histograms indicate means of the MFIs, normalized to Foxp3$^-$ CD4$^+$ CD44^{lo} T cells of *Tcra*$^{F/F}$ mice. Means were calculated from $\geq$ 5 mice per genotype from $\geq$ 2 independent experiments. Bars indicate medians. ***p < 0.001; **p < 0.01; one-way ANOVA.

(C) Differences in mRNA expression amounts of the indicated enzymes of the cholesterol biosynthesis pathway normalized to Ywhaz relative to Foxp3$^-$ CD4$^+$ conventional T cells (dotted line). Bars indicate means + SD from 3 samples (one mouse per sample for Foxp3$^-$ CD4$^+$ T cells and TCR$^+$ CD25^{hi} Foxp3$^+$ Treg cells and 3 mice pooled per sample for TCR$^-$ CD25^{hi} Foxp3$^+$ Treg cells). See also Figure S5.

we did not observe enhanced FoxO1-dependent gene expression in TCR$^-$ Treg cells (Figure S5G). Therefore, it is also possible that the observed Bim/Bcl-2 balance is caused by absent repression of Bcl-2 through complexes containing c-Maf and c-Myb (Peng et al., 2007), as both are strongly reduced after TCR ablation (Figures 2C and S3A).

Our results provide correlative evidence that in the absence of continuous TCR stimulation, signaling through the mTORC1 and mTORC2 pathways is attenuated in Treg cells. Although we detected only minor effects in downstream gene expression, these pathways still might be important to keep target genes in a poised state for rapid expression upon strong Treg cell stimulation.

TCR-Deficient Treg Cells Lose Most of Their Suppressive Protein Arsenal and Their Ability to Suppress T Cell Responses In Vivo

Various mechanisms are implicated in the suppressive ability of Treg cells (Josefowicz et al., 2012; Sakaguchi et al., 2008; Shevach, 2009). Among them are the consumption of the cytokine IL-2, the release of suppressive cytokines (IL-10, IL-35 [composed of p35 and Ebi3] and TGF-β) or toxic molecules (perforin, granzymes), and the modulation of the costimulatory abilities of antigen-presenting cells.

Gene-expression analysis of 10 1.5-fold or more regulated putative suppressor genes revealed that 8 were downregulated and 2 (Perforin and CD274) were upregulated in TCR-deficient Treg cells (Figures 6A and S6A). Verification of these and analysis of further candidates by flow cytometry and/or real-time PCR (Figures 6B and 6C) revealed that of the 20 putative suppressor genes tested, 59% (13) were significantly downregulated upon TCR ablation (Figures 6D and S6A): *Nt5e* (CD73), *Ctla4*, *Ebi3*, *Fgl2*, *Tnfrsf18* (GITR), *Il10*, *Il10r*, *Lag3*, *Tgfb1* (latency associated peptide, LAP), *Itgal* (LFA-1), *Nrp1*, *Pdcd1lg2* (PD-L2), and *Tigit*.

In line with reduced *Il10* mRNA expression, a significantly smaller percentage of TCR$^-$ Treg cells produced IL-10 after PMA and Ionomycin activation in vitro in comparison to their TCR$^+$ counterparts (Figures 6E and S6B). Importantly,

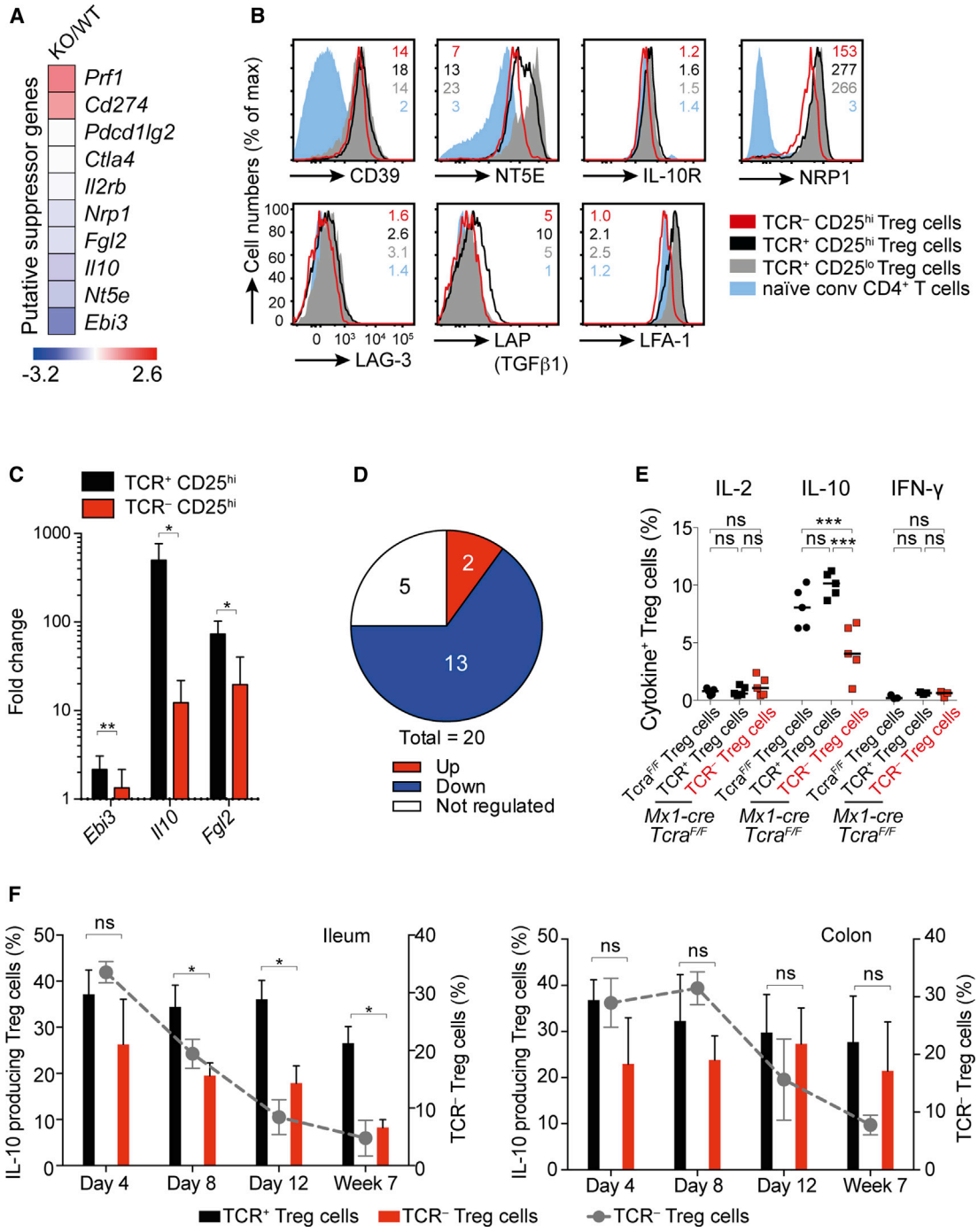

Figure 6. Regulatory T Cells Show Reduced Expression of Several Important Suppressive Molecules

(A) Heatmap showing mRNA expression of the indicated 1.5-fold regulated suppressive markers of TCR$^+$ versus TCR$^-$ Foxp3$^+$ Treg cells, 6 weeks after poly(I:C) injection, analyzed by Affymetrix microarray.

(B) Extracellular expression of the depicted markers of the indicated splenic T cell subsets (Treg = Foxp3$^+$), all from *Mx1-cre Tcra*$^{F/F}$ mice, 6 weeks after poly(I:C) injection. Numbers in representative histograms indicate means of the median fluorescence intensities (MFIs), normalized to Foxp3$^-$ CD4$^+$ CD44^{lo} naive T cells of *Tcra*$^{F/F}$ mice. Means were calculated from ≥ 5 mice per genotype from ≥ 2 independent experiments.

(C) Differences in mRNA expression amounts of the indicated suppressive markers normalized to Ywhaz relative to Foxp3$^-$ CD4$^+$ T cells (dotted line). Bars indicate means + SD from 3 samples (one mouse per replicate for Foxp3$^-$ CD4$^+$ T cells and CD25^{hi} Foxp3$^+$ TCR Treg cells and 3 mice pooled per replicate for TCR$^-$ CD25^{hi} Foxp3$^+$ Treg cells). **p < 0.01; *p < 0.05; t test.

(D) Regulation of 20 putative suppressive molecules in KO relative to WT Treg cells on the mRNA and/or protein amount (white, not regulated; red, upregulated, blue, downregulated).

(legend continued on next page)

TCR-deficient Treg cells kept their anergic phenotype in respect to IL-2 (and interferon-γ [IFN-γ]) production upon activation (Figures 6E and S6B). After TCR ablation the proportion of TCR$^-$ Treg cells in the gut lamina propria decreased progressively (Figure 6F). In the ileum, a significantly smaller proportion of TCR$^-$ Treg cells produced IL-10 from day 8 onward. Conversely, in the colon, TCR$^-$ Treg cells largely maintained their ability to secrete IL-10 (Figures 6F and S6C). This indicates that the cytokine and/or costimulation milieu in the colon can at least partially substitute antigenic signals with regards to IL-10 production, but not to cellular homeostasis. We therefore conclude that, overall, the expression of suppressive genes by Treg cells largely depends on constant TCR signals, even though specific niches might maintain suppressive functions in absence of antigenic triggers.

To test the consequences of Treg cell TCR ablation in an in vivo setting, we employed CD4-CreER^{T2} animals (Sledzińska et al., 2013) because of the higher recombination efficiencies in mature T cells compared to *Mx1-cre* mice. Application of 3 or 5 mg tamoxifen for 5 consecutive days leads to loss of the TCR on around 70% of peripheral Treg cells (Figure S7A). We reconstituted T cell-deficient mice with naive T cells together with Treg cells isolated from either *Tcra*$^{F/F}$ control or CD4-CreER^{T2} *Tcra*$^{F/F}$ animals (Figure S7B). In the context of T cell deficiency, these cells rigorously expand. Three weeks after adoptive transfer, TCR ablation was induced through tamoxifen treatment (Figure 7A). Three days after cessation of tamoxifen feeding, we confirmed TCR ablation in 67% and 55% of CD4-CreER^{T2} *Tcra*$^{F/F}$ Treg cells present in the spleen and mesenteric lymph nodes, respectively (Figure S7C). The tamoxifen treatment induced a transient weight loss in all cohorts. However, while the control animals quickly recovered after cessation of tamoxifen feeding, we observed significantly reduced weight gain in animals in which we ablated the TCR on Treg cells (Figure 7B). Two of nine experimental animals developed diarrhea and signs of colitis with severe cellular infiltrations and associated inflammation (Figure S7D; data not shown). Furthermore, we noticed increased spleen and mesenteric lymph node weights, indicating ongoing inflammation, 24 days after TCR ablation on Treg cells (Figure 7C). This was partially due to infiltration of eosinophils, monocytes, and/or macrophages, as well as neutrophils in both organs (Figures 7D and S7E). At this time point, total Treg cell counts, of which 20% were TCR-deficient, were slightly increased in Treg cell TCR ablated animals, indicating a strong compensatory proliferation of TCR$^+$ Treg cells. The number of pTreg cells was not increased (Figure S7F). However, the initial yet transient presence of over 50% of TCR-deficient Treg cells was sufficient to disrupt normal immune homeostasis. Importantly, we also observed strongly increased numbers of CD4$^+$ T cells (Figure 7E), which showed an activated phenotype as indicated by increased CD69 expression (Figure 7F). Among the significantly expanded CD4$^+$ T cell subsets were T helper 17 (Th17) cells (Figure 7G) that are commonly connected to autoimmunity and inflammatory disease settings and are under strict control of regulatory T cells (Josefowicz et al., 2012). Reduced production of IL-10 also could contribute to disease development. In a similar experiment in *Rag2*$^{-/-}$ mice (Figures S7G–S7J), we did not observe differences in weight (data not shown), likely due to lower TCR ablation efficiencies (Figure S7H). However, TCR ablation exacerbated intestinal pathology (Figure S7I) and significantly increased numbers of splenocytes, including CD4$^+$ T cells (Figure S7J).

In order to test conditional Treg cell TCR ablation in an autoimmune disease setting with an unmanipulated effector T cell compartment, we used an experimental autoimmune encephalomyelitis (EAE) model (Figure 7H). Here, we transiently erased the Foxp3$^+$ Treg cell compartment by diphtheria toxin injections in DEREG mice and replenished the peripheral Treg cell niche with in vitro expanded control Treg cells (*Tcra*$^{F/F}$) or Treg cells with a tamoxifen-ablatable TCR (CD4-CreER^{T2} *Tcra*$^{F/F}$) (Figure S7K). Upon immunization with $MOG_{35–55}$ in complete Freund's adjuvant (CFA), we found that mice that received Treg cells whose TCR was ablated in vivo 6 days after immunization developed more severe EAE and behaved like mice who did not receive Treg cells after depletion of endogenous Treg cells (Figure 7I). The expansion of endogenous Treg cells, which is typical of the DEREG model, most likely masks the effects of TCR ablation at later time points after EAE induction. We obtained similar results when a higher number of Treg cells were transferred (Figures 7J and S7L and S7M).

Altogether, these results strongly support the notion that in the absence of continuous TCR signaling, Treg cells lose their ability to control normal immune homeostasis and to suppress autoimmune reactions.

DISCUSSION

Treg cells can be broadly separated into two different subsets in vivo. Naive, slowly cycling Treg cells and the effector subset, which is composed of highly proliferative cells characterized by a generally more activated state, likely due to recent autoantigen recognition. In line with this hypothesis, six weeks after TCR ablation we failed to detect TCR-deficient Treg cells expressing any of the characteristic activated or effector T cell markers, even though initial TCR ablation in these subsets was as efficient as in naive Treg cells. Our data thus clearly demonstrate that effector Treg cells cannot be generated or maintained in absence of TCR signals.

We propose that TCR-independent hypomethylation and Foxp3 expression in conjunction with other unaffected transcription factors largely ensure continued identity of TCR$^-$ Treg cells. Nevertheless, a large proportion of the Treg cell-defining gene expression, including Foxp3-regulated genes, depended on TCR signals to varying degrees. This might be explained by a differential dependence on strictly TCR controlled transcription factors such as Egr2, c-Maf, and c-Rel, and possibly also factors

(E) Percentages of splenic Foxp3$^+$ Treg cells expressing IL-2, IL-10, or IFN-γ upon in vitro activation with PMA and Ionomycin for 5 hr. Cells were extracted from mice and activated 6 weeks after poly(I:C) injection. Bars indicate medians. ***$p < 0.001$; ns, not significant; one-way ANOVA.
(F) Percentages of TCR$^-$ Treg cells of total Treg cells isolated from the gut lamina propria of *Mx1-cre Tcra*$^{F/F}$ mice at the indicated time points after poly(I:C) injection (right y axis). After stimulation with PMA and Ionomycin IL-10 production was assessed in TCR$^-$ CD25^{hi} and TCR$^+$ CD25^{hi} Foxp3$^+$ Treg cells (left y axis). Bars indicate means ± SD that were calculated from ≥ 3 mice per time point. *$p < 0.05$; ns, not significant; t test. See also Figure S6.

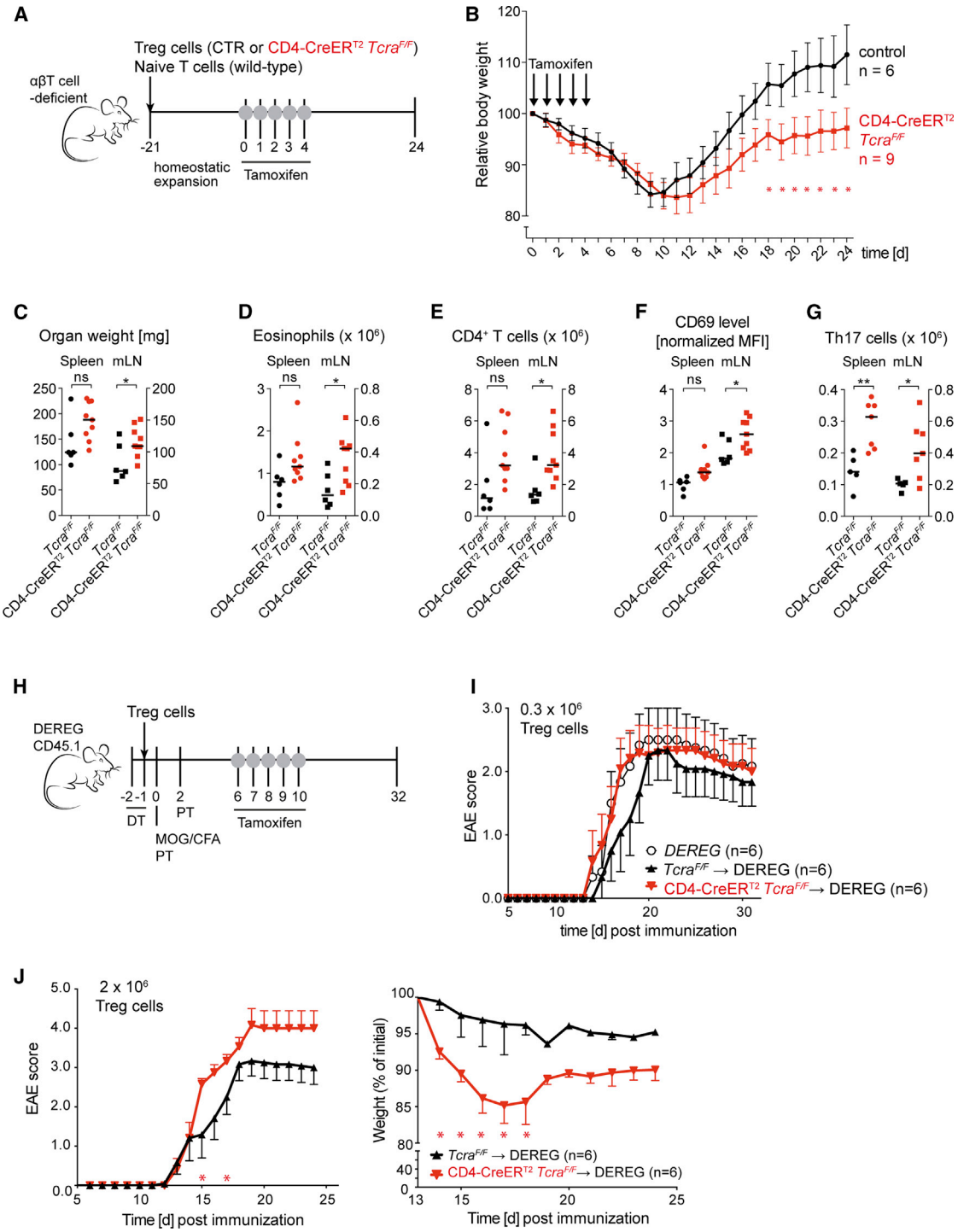

Figure 7. In Vivo TCR Ablation of Treg Cells Leads to Inflammation

(A–G) T cell-deficient *Tcra*$^{-/-}$ mice were reconstituted with Foxp3-I-eGFP$^-$ naive T cells together with CD4$^+$ CD25^{hi} Treg cells from either *Tcra*$^{F/F}$ control or from CD4-CreER^{T2} *Tcra*$^{F/F}$ mice. After 3 weeks of engraftment, TCR ablation was induced through tamoxifen feeding. Twenty-four days later, animals were sacrificed and analyzed.

(B) Body weight of the animals, normalized to the respective weight on the first day of tamoxifen treatment. Shown are means ± SEM; SEM are shown for visual clarity; *p < 0.05; t test.

(C) Weight of the indicated organs. Bars indicate medians. *p < 0.05; ns, not significant; one-way ANOVA.

(D, E, and G) Total cell numbers of (D) eosinophils (CD11c$^-$ CD11b$^+$ SiglecF$^+$ SSC-A^{hi}); (E) CD4$^+$ T cells (TCRβ$^+$ CD5$^+$); (G) Th17 T cells (Ror-γt$^+$ CD4$^+$ TCRβ$^+$ CD5$^+$). Bars indicate medians. **p < 0.01; *p < 0.05; ns, not significant; one-way ANOVA.

(legend continued on next page)

of the NFAT family. Surprisingly, target gene analysis pointed to IRF4 as a critical mediator of TCR-induced gene expression, although its protein amounts were only moderately affected by TCR loss. This indicated a critical role for TCR signals in controlling IRF4 activity in Treg cells, directly or through its transcriptional coregulators. We also found that loss of TCR signals correlated with a reduction of mTORC1 and mTORC2 activity in Treg cells to an amount comparable to naive $CD4^+$ T cells.

With respect to homeostatic maintenance, TCR^- Treg cells behaved identically to TCR^- naive $CD4^+$ T cells. In striking contrast to memory T and NKT cells (Polic et al., 2001; Vahl et al., 2013), TCR signals were indispensable for the proliferation of Treg cells under steady-state conditions in vivo. In the absence of thymic output, this nondividing pool of TCR-deficient Treg cells was reduced to half its size in 46 days, corresponding to a Treg cell loss of around 1.5% per day. Because directly ex vivo isolated TCR-deficient Treg cells were as viable as their TCR-proficient counterparts, this indicates that the decay of TCR-deficient Treg cells in vivo was not due to enhanced cell death but due to essentially abolished proliferation. The protein amounts of and balance between pro- (Bim) and anti-apoptotic (Bcl-2) proteins in TCR^- Treg cells resembled those found in naive $CD4^+$ T cells and were markedly different from TCR^+ Treg cells. Potential mechanisms for this phenomenon are attenuated AKT and mTORC2 signaling and/or other transcriptional regulation. Upon egress from the thymus, regulation of peripheral Treg cell homeostasis has been mainly attributed to cytokine signaling (Setoguchi et al., 2005). Conversely, we found that the homeostasis of TCR-deficient Treg cells was strongly impaired even though they expressed normal amounts of cytokine receptors for IL-2, IL-7, and IL-15 and signaled normally in response to IL-2 or IL-6 stimulation. Instead, our results suggest that constant TCR triggering constitutes an obligate prerequisite. It should be mentioned that in our experimental system, Cre-mediated TCR ablation in Treg cells is not complete, and therefore TCR-deficient Treg cells are competing with TCR-expressing cells. It is possible that the homeostatic defects of TCR-deficient Treg cells are confounded by this competition.

Loss of individual suppressive proteins in Treg cells does not match the dramatic phenotype of Foxp3-deficiency. Thus, depending on the type of immune response and the location in the body, several different suppression mechanisms are important. Still, it is not well understood how Treg cell TCR engagement is involved in suppression of target cells. At least in vitro, directly ex vivo isolated Treg cells are able to suppress without previous activation (Szymczak-Workman et al., 2009). It has been speculated that autoantigen recognition is key to maintain polyclonal Treg cells in an activated state, allowing them to control various different immune responses independently of TCR specificity (Shevach, 2009). Our data imply that TCR signals are absolutely required for the differentiation and maintenance of effector Treg subsets, which is critical for effective control of overshooting autoimmune or inflammatory responses in various disease contexts. Furthermore, in naive Treg cells, constant TCR triggers ensure high expression of most suppressive proteins. Treg cell TCR ablation in two in vivo models resulted in increased clinical effects, despite the fact that Treg cell TCR ablation remained incomplete at around 50%–70%. One possibility is that TCR^- Treg cells are unable to suppress but still occupy homeostatic niches and thereby impede the action of TCR^+ Treg cells.

In summary, our study demonstrates that Treg cells continuously receive biologically relevant signals through their autoreactive TCR and that these signals are essential for Treg cell homeostasis, signature gene expression, and especially for their suppressive functions. By ablating the TCR, we abolished MHCII recognition and (auto-)antigenic stimulation, and it is likely that both deficiencies contribute to varying degrees to the effects we observe. Future studies should aim at dissecting these individual contributions. In essence, our study solidifies the view of the Treg cell population as a constantly TCR-activated T cell subset whose activation is channeled into suppression through the actions of Foxp3.

EXPERIMENTAL PROCEDURES

Genetically Modified Mice

Mx1-cre (Kühn et al., 1995), $Tcra^F$ and $Tcra^-$ ($Tcra^{tm1Cgn}$; Polic et al., 2001), Foxp3-I-eGFP (Bettelli et al., 2006), CD4-$CreER^{T2}$ (Sledzińska et al., 2013), $Gt(ROSA)26Sor^{tm4(ACTB-tdTomato,-EGFP)Luo}/J$ (mT/mG; Muzumdar et al., 2007), and CD45.1-congenic DEREG (Lahl et al., 2007) mice were all kept on a C57BL/6 genetic background. Six- to eight-week-old *Mx1-cre* $Tcra^{F/F}$ or $Tcra^{F/F}$ mice were given a single dose (400 μg) of poly(I:C) (Amersham). All mice were analyzed 6 weeks later, unless otherwise indicated. Mice were housed in specific pathogen-free animal facilities of the MPIB and the Technische Universität München. All animal procedures were approved by the Regierung of Oberbayern.

Flow Cytometry

Single-cell suspensions were prepared and stained with the antibodies listed under Supplemental Experimental Procedures.

BrdU Incorporation

Mice were fed with 0.5 mg/mL BrdU (Sigma) in the drinking water for 4 consecutive weeks, and BrdU incorporation was measured with the BrdU Flow Kit (BD).

Cell Sorting and Gene-Expression Analysis

TCR^+ ($Foxp3^+$ $CD4^+$ $CD25^{hi}$ cells from $Tcra^{F/F}$ Foxp3-I-eGFP mice) and TCR^- ($Foxp3^+$ TCR^- $CD4^+$ $CD25^{hi}$ cells from *Mx1-cre* $Tcra^{F/F}$ Foxp3-I-eGFP mice) Treg cells were sorted 6 weeks after poly(I:C) injection with a FACSAria (BD). Cells from three to five mice were pooled for sorting one replicate, and four replicates for the controls as well as five replicates for the *Mx1-cre* $Tcra^{F/F}$ Foxp3-I-eGFP mice were generated. mRNA from 3–5 × 10^5 cells was purified with a RNeasy Micro kit (QIAGEN), amplified, labeled, and

(F) CD69 expression on $CD4^+$ T cells. Scatterplots show means of the MFIs, normalized to splenic $CD4^+$ T cells of control mice. *$p < 0.05$; ns, not significant; one-way ANOVA.

(H) Scheme of EAE experiment: DEREG mice were depleted of endogenous Treg cells by diphtheria toxin and then left unreconstituted (DEREG) or reconstituted with control ($Tcra^{F/F}$ → DEREG) or TCR ablatable $CD4^+$ $CD25^{hi}$ Treg cells (CD4-$CreER^{T2}$ $Tcra^{F/F}$ → DEREG) followed by induction of EAE.

(I and J) EAE experiment with 3 × 10^5 (I) or 2 × 10^6 (J) adoptively transferred $Tcra^{F/F}$ or CD4-$CreER^{T2}$ $Tcra^{F/F}$ $CD4^+$ $CD25^{hi}$ Treg cells or DEREG mice that were left unreconstituted. Mean clinical disease scores ± SEM of the indicated groups (n = 6) are shown on the left. SEM is shown for visual clarity. *$p < 0.05$; Mann-Whitney U test. Body weight, shown on the right, was normalized to the first measured weight of the respective animal; *$p < 0.05$; t test. See also Figure S7.

hybridized to Affymetrix M430 V2 microarrays (Geo: microarray data, GSE62532). Array normalization and expression value calculation was performed using DNA-Chip Analyzer (www.dchip.org). Heatmaps were generated with GenePattern Software. Gene set enrichment analysis (GSEA) was performed at http://www.broadinstitute.org/gsea/index.jsp. RNA from sorted cells was isolated (QIAGEN) and reverse transcribed (Promega) for qRT-PCR with Universal Probe Library probes and primers (Roche Diagnostics).

CpG Methylation Analysis by Bisulfite Sequencing

TCR^+ and TCR^- Treg cells were sorted 6 weeks and 15 weeks after poly(I:C) injection as for the gene expression analysis. Control tTreg and iTreg cells were generated, and the CpG methylation status was analyzed, as previously described (Ohkura et al., 2012).

In Vivo Suppression Assays

T cell-deficient *Tcra*$^{-/-}$ mice at the age of 6–8 weeks were reconstituted with 1×10^6 naive $CD4^+$ T cells (Foxp3-I-eGFP$^-$ $CD45RB^{hi}$ $CD25^-$) together with 0.25×10^6 Treg cells ($CD4^+$ $CD25^{hi}$ $CD45RB^{int}$ $CD38^{hi}$) from either CD4-CreER^{T2} *Tcra*$^{F/F}$ or littermate control mice. Starting 3 weeks after cell transfer, mice were fed per os with 5 mg tamoxifen per day (Sigma) for 5 consecutive days, and their weight was monitored. Colon samples were fixed in 4% paraformaldehyde, embedded in paraffin, sectioned, and stained with hematoxylin and eosin. For the EAE model, endogenous DEREG CD45.1 Treg cells were depleted by injection of 500 ng diphtheria toxin (Calbiochem) on days −2 and −1 prior to immunization and substituted by 0.3×10^6 or 2×10^6 Treg cells obtained from either CD4-CreER^{T2} *Tcra*$^{F/F}$ or littermate controls. EAE was induced by s.c. immunization with 200 μg of MOG35-55 (Auspep) in CFA containing 500 μg *M. tuberculosis* H37Ra (Difco) plus intravenous injection of 200 ng pertussis toxin (Sigma) on days 0 and 2 after immunization. Starting on day 5 postimmunization, mice were fed with tamoxifen (Hexal) in ClinOleic 20% (Baxter) for 5 consecutive days (0.15 mg/g ≈3 mg/mouse on day 5 and 0.10 mg/g ≈2 mg/mouse on the following days). Disease progress and severity were assessed as published (Korn et al., 2007).

Statistics

Statistical analysis of the results was performed by one-way ANOVA followed by Tukey's test, by Student's t test as indicated. p values are presented in figure legends where a statistically significant difference was found. EAE scores between groups were analyzed as disease burden per individual day with Mann-Whitney U test.

ACCESSION NUMBER

The GEO accession number for the microarray data reported in this paper is GSE62532.

SUPPLEMENTAL INFORMATION

Supplemental Information includes seven figures, two tables, and Supplemental Experimental Procedures and can be found with this article online at http://dx.doi.org/10.1016/j.immuni.2014.10.012.

AUTHOR CONTRIBUTIONS

J.C.V. and C.D. designed, performed, and analyzed most experiments and wrote the manuscript; K.H., S.H., J.C.F., J.N., N.O., D.R., T.B., B.P., L.K., T.K., A.S., and S.S. designed, performed, and analyzed experiments; H.M., S.S., M.Y.H., R.Z., A.S.-G., and K.K. analyzed experiments; M.S.-S. conceptualized the work, directed the study, analyzed data, and wrote the manuscript.

ACKNOWLEDGMENTS

This study was supported by the DFG through SFB 1054 TPA02 and an Emmy Noether grant to M.S.-S. J.C.V. and K.H. received PhD stipends from the Ernst Schering Foundation and the Boehringer Ingelheim Fonds, respectively. T.K. is supported by the DFG (Heisenberg, SFB 1054 TPB06, and SyNergy). We are grateful to R. Fässler for support. We thank J. Knogler, B. Habermehl, M. Schmickl, and A. Kawasaki for technical assistance.

Received: May 5, 2014
Accepted: October 22, 2014
Published: November 6, 2014

REFERENCES

Bensinger, S.J., Bandeira, A., Jordan, M.S., Caton, A.J., and Laufer, T.M. (2001). Major histocompatibility complex class II-positive cortical epithelium mediates the selection of CD4(+)25(+) immunoregulatory T cells. J. Exp. Med. *194*, 427–438.

Bettelli, E., Carrier, Y., Gao, W., Korn, T., Strom, T.B., Oukka, M., Weiner, H.L., and Kuchroo, V.K. (2006). Reciprocal developmental pathways for the generation of pathogenic effector TH17 and regulatory T cells. Nature *441*, 235–238.

Campbell, D.J., and Koch, M.A. (2011). Phenotypical and functional specialization of FOXP3+ regulatory T cells. Nat. Rev. Immunol. *11*, 119–130.

Chi, H. (2012). Regulation and function of mTOR signalling in T cell fate decisions. Nat. Rev. Immunol. *12*, 325–338.

Darrasse-Jèze, G., Deroubaix, S., Mouquet, H., Victora, G.D., Eisenreich, T., Yao, K.-H., Masilamani, R.F., Dustin, M.L., Rudensky, A., Liu, K., and Nussenzweig, M.C. (2009). Feedback control of regulatory T cell homeostasis by dendritic cells in vivo. J. Exp. Med. *206*, 1853–1862.

del Peso, L., González-García, M., Page, C., Herrera, R., and Nuñez, G. (1997). Interleukin-3-induced phosphorylation of BAD through the protein kinase Akt. Science *278*, 687–689.

Feuerer, M., Hill, J.A., Mathis, D., and Benoist, C. (2009). Foxp3+ regulatory T cells: differentiation, specification, subphenotypes. Nat. Immunol. *10*, 689–695.

Fisson, S., Darrasse-Jèze, G., Litvinova, E., Septier, F., Klatzmann, D., Liblau, R., and Salomon, B.L. (2003). Continuous activation of autoreactive CD4+ CD25+ regulatory T cells in the steady state. J. Exp. Med. *198*, 737–746.

Fontenot, J.D., Rasmussen, J.P., Williams, L.M., Dooley, J.L., Farr, A.G., and Rudensky, A.Y. (2005). Regulatory T cell lineage specification by the forkhead transcription factor foxp3. Immunity *22*, 329–341.

Fu, W., Ergun, A., Lu, T., Hill, J.A., Haxhinasto, S., Fassett, M.S., Gazit, R., Adoro, S., Glimcher, L., Chan, S., et al. (2012). A multiply redundant genetic switch 'locks in' the transcriptional signature of regulatory T cells. Nat. Immunol. *13*, 972–980.

Hedrick, S.M., Hess Michelini, R., Doedens, A.L., Goldrath, A.W., and Stone, E.L. (2012). FOXO transcription factors throughout T cell biology. Nat. Rev. Immunol. *12*, 649–661.

Huehn, J., Siegmund, K., Lehmann, J.C.U., Siewert, C., Haubold, U., Feuerer, M., Debes, G.F., Lauber, J., Frey, O., Przybylski, G.K., et al. (2004). Developmental stage, phenotype, and migration distinguish naive- and effector/memory-like CD4+ regulatory T cells. J. Exp. Med. *199*, 303–313.

Jorgensen, T.N., McKee, A., Wang, M., Kushnir, E., White, J., Refaeli, Y., Kappler, J.W., and Marrack, P. (2007). Bim and Bcl-2 mutually affect the expression of the other in T cells. J. Immunol. *179*, 3417–3424.

Josefowicz, S.Z., Lu, L.-F., and Rudensky, A.Y. (2012). Regulatory T cells: mechanisms of differentiation and function. Annu. Rev. Immunol. *30*, 531–564.

Kim, J.K., Klinger, M., Benjamin, J., Xiao, Y., Erle, D.J., Littman, D.R., and Killeen, N. (2009). Impact of the TCR signal on regulatory T cell homeostasis, function, and trafficking. PLoS ONE *4*, e6580.

Koonpaew, S., Shen, S., Flowers, L., and Zhang, W. (2006). LAT-mediated signaling in CD4+CD25+ regulatory T cell development. J. Exp. Med. *203*, 119–129.

Korn, T., Reddy, J., Gao, W., Bettelli, E., Awasthi, A., Petersen, T.R., Bäckström, B.T., Sobel, R.A., Wucherpfennig, K.W., Strom, T.B., et al. (2007). Myelin-specific regulatory T cells accumulate in the CNS but fail to control autoimmune inflammation. Nat. Med. *13*, 423–431.

Kühn, R., Schwenk, F., Aguet, M., and Rajewsky, K. (1995). Inducible gene targeting in mice. Science *269*, 1427–1429.

Lahl, K., Loddenkemper, C., Drouin, C., Freyer, J., Arnason, J., Eberl, G., Hamann, A., Wagner, H., Huehn, J., and Sparwasser, T. (2007). Selective depletion of Foxp3+ regulatory T cells induces a scurfy-like disease. J. Exp. Med. *204*, 57–63.

Moran, A.E., Holzapfel, K.L., Xing, Y., Cunningham, N.R., Maltzman, J.S., Punt, J., and Hogquist, K.A. (2011). T cell receptor signal strength in Treg and iNKT cell development demonstrated by a novel fluorescent reporter mouse. J. Exp. Med. *208*, 1279–1289.

Morikawa, H., Ohkura, N., Vandenbon, A., Itoh, M., Nagao-Sato, S., Kawaji, H., Lassmann, T., Carninci, P., Hayashizaki, Y., Forrest, A.R.R., et al.; FANTOM Consortium (2014). Differential roles of epigenetic changes and Foxp3 expression in regulatory T cell-specific transcriptional regulation. Proc. Natl. Acad. Sci. USA *111*, 5289–5294.

Muzumdar, M.D., Tasic, B., Miyamichi, K., Li, L., and Luo, L. (2007). A global double-fluorescent Cre reporter mouse. Genesis *45*, 593–605.

Ohkura, N., Hamaguchi, M., Morikawa, H., Sugimura, K., Tanaka, A., Ito, Y., Osaki, M., Tanaka, Y., Yamashita, R., Nakano, N., et al. (2012). T cell receptor stimulation-induced epigenetic changes and Foxp3 expression are independent and complementary events required for Treg cell development. Immunity *37*, 785–799.

Peng, S., Lalani, S., Leavenworth, J.W., Ho, I.-C., and Pauza, M.E. (2007). c-Maf interacts with c-Myb to down-regulate Bcl-2 expression and increase apoptosis in peripheral CD4 cells. Eur. J. Immunol. *37*, 2868–2880.

Polic, B., Kunkel, D., Scheffold, A., and Rajewsky, K. (2001). How alpha beta T cells deal with induced TCR alpha ablation. Proc. Natl. Acad. Sci. USA *98*, 8744–8749.

Rudra, D., deRoos, P., Chaudhry, A., Niec, R.E., Arvey, A., Samstein, R.M., Leslie, C., Shaffer, S.A., Goodlett, D.R., and Rudensky, A.Y. (2012). Transcription factor Foxp3 and its protein partners form a complex regulatory network. Nat. Immunol. *13*, 1010–1019.

Sakaguchi, S., Yamaguchi, T., Nomura, T., and Ono, M. (2008). Regulatory T cells and immune tolerance. Cell *133*, 775–787.

Setoguchi, R., Hori, S., Takahashi, T., and Sakaguchi, S. (2005). Homeostatic maintenance of natural Foxp3(+) CD25(+) CD4(+) regulatory T cells by interleukin (IL)-2 and induction of autoimmune disease by IL-2 neutralization. J. Exp. Med. *201*, 723–735.

Shevach, E.M. (2009). Mechanisms of foxp3+ T regulatory cell-mediated suppression. Immunity *30*, 636–645.

Siggs, O.M., Miosge, L.A., Yates, A.L., Kucharska, E.M., Sheahan, D., Brdicka, T., Weiss, A., Liston, A., and Goodnow, C.C. (2007). Opposing functions of the T cell receptor kinase ZAP-70 in immunity and tolerance differentially titrate in response to nucleotide substitutions. Immunity *27*, 912–926.

Sledzińska, A., Hemmers, S., Mair, F., Gorka, O., Ruland, J., Fairbairn, L., Nissler, A., Müller, W., Waisman, A., Becher, B., and Buch, T. (2013). TGF-β signalling is required for $CD4^+$ T cell homeostasis but dispensable for regulatory T cell function. PLoS Biol. *11*, e1001674.

Stephens, G.L., Andersson, J., and Shevach, E.M. (2007). Distinct subsets of FoxP3+ regulatory T cells participate in the control of immune responses. J. Immunol. *178*, 6901–6911.

Szymczak-Workman, A.L., Workman, C.J., and Vignali, D.A.A. (2009). Cutting edge: regulatory T cells do not require stimulation through their TCR to suppress. J Immunol *182*, 5188–5192.

Vahl, J.C., Heger, K., Knies, N., Hein, M.Y., Boon, L., Yagita, H., Polic, B., and Schmidt-Supprian, M. (2013). NKT cell-TCR expression activates conventional T cells in vivo, but is largely dispensable for mature NKT cell biology. PLoS Biol. *11*, e1001589.

Xing, Y., and Hogquist, K.A. (2012). T-cell tolerance: central and peripheral. Cold Spring Harb. Perspect. Biol. *4*, a007021–a007021.

Zeng, H., Yang, K., Cloer, C., Neale, G., Vogel, P., and Chi, H. (2013). mTORC1 couples immune signals and metabolic programming to establish T(reg)-cell function. Nature *499*, 485–490.